Title

The Kolmogorov-Obukhov Statistical Theory of Turbulence

Author
Birnir, Bjorn

Publication Date
2012-10-15

The Kolmogorov-Obukhov Statistical Theory of Turbulence

Björn Birnir

Center for Complex and Nonlinear Science
and
Department of Mathematics
University of California, Santa Barbara

October 15, 2012

In 1941 Kolmogorov and Obukhov proposed that there exists a statistical theory of turbulence that should allow the computation of all the statistical quantities that can be computed and measured in turbulent systems. These are quantities such as the moments, the structure functions and the probability density functions (PDFs) of the turbulent velocity field. In this paper we will outline how to construct this statistical theory from the stochastic Navier-Stokes equation. The additive noise in the stochastic Navier-Stokes equation is generic noise given by the central limit theorem and the large deviation principle. The multiplicative noise consists of jumps multiplying the velocity, modeling jumps in the velocity gradient. We first estimate the structure functions of turbulence and establish the Kolmogorov-Obukhov '62 scaling hypothesis with the She-Leveque intermittency corrections. Then we compute the invariant measure of turbulence writing the stochastic Navier-Stokes equation as an infinite-dimensional Ito process and solving the linear Kolmogorov-Hopf functional differential equation for the invariant measure. Finally we project the invariant measure onto the PDF. The PDFs turn out to be the normalized inverse Gaussian (NIG) distributions of Barndorff-Nilsen, and compare well with PDFs from simulations and experiments.

1 Introduction

In 1941 Kolmogorov and Obukhov [21, 20, 27] proposed a statistical theory of turbulence based on dimensional arguments. The main consequence and test of this theory was that the structure functions of the velocity differences of a turbulent fluid

$$E(|u(x,t)-u(x+l,t)|^p) = S_p = C_p l^{p/3}$$

should scale with the distance (lag variable) l between them, to the power $p/3$. This theory was immediately criticized by Landau for not taking into account the influence of the large flow structure on the constants C_p and later for not including the influence of the intermittency in the velocity fluctuations on the scaling exponents.

In 1962 Kolmogorov and Obukhov [22, 28] proposed a corrected theory were both of those issues were addressed. They also pointed out that the scaling exponents for the first two structure functions could be corrected by log-normal processes. For higher order structure functions the log-normal processes gave intermittency corrections inconsistent with contemporary simulations and experiments, see [1].

The correct intermittency corrections were found by She and Leveque [35] in 1994. She and Waymire [36] and Dubrulle [16] showed that these corrections are produced by log-Poisson processes.

Assuming that the noise in fully-developed turbulence is a generic noise determined by the general theorems in probability, the central limit theorem and the large deviation principle, we are able to formulate and solve the Kolmogorov-Hopf equation for the invariant measure of the stochastic Navier-Stokes equations. The stochastic Navier-Stokes equation arises from the deterministic equation when fluid instabilities magnify ambient noise present in the fluid, see [11]. It can also be considered to be the equation for the small (inertial) scales in a Reynolds decomposition, [8, 32] of the flow, or the equation for the small scales in a coarse graining of the Navier-Stokes equation, see [23].

The intermittency corrections to the scaling exponents of the structure functions require a multiplicative (multipling the fluid velocity u) noise in the stochastic Navier-Stokes equation. We let this multiplicative noise, in the equation, consists of a simple (Poisson) jump process and then show how the Feynmann-Kac formula produces the log-Poissonian processes, see [35], [36] and [16], in the solution. These log-Poissonian processes give the intermittency corrections that agree with modern direct Navier-Stokes simulations (DNS) and experiments.

The probability density function (PDF) plays a key role when direct Navier-Stokes simulations or experimental results are compared to theory. The statistical theory of turbulence is determined, including the scaling of the structure functions of turbulence, by the invariant measure of the Navier-Stokes equation and the PDFs for the various statistics (one-point, two-point,$\cdots$, N-point) can be obtained by taking the trace of the corresponding invariant measures. Hopf [18] derived a functional equation for the characteristic function (Fourier transform) of the invariant measure. In distinction to the nonlinear Navier-Stokes equation, this is a *linear* functional differential equation. The theory for solving such equation, see Da Prato [33], has only recently become available.

The PDFs obtained from the invariant measures for the velocity differences (two-point statistics) are shown to be the four parameter normalized inverse Gaussian (NIG) distributions, found and investigated by Barndorff-Nilsen [4, 5]. These PDF have heavy tails and a convex peak at the origin. A suitable projection of the Kolmogorov-Hopf equations is the differential equation determining the NIG distributions. Because of intermittency each structure function generates its own NIG distribution with separate parameters. Then we compare these PDFs with DNS results and experimental data, see also [6, 7].

2 The Deterministic Navier-Stokes Equation

Fluid flow is described by the deterministic Navier-Stokes equation

$$\begin{aligned} u_t + u \cdot \nabla u &= \nu \Delta u - \nabla p \\ u(x,0) &= u_0(x) \end{aligned} \tag{1}$$

with the incompressibility conditions

$$\nabla \cdot u = 0, \tag{2}$$

where $u(x)$, $x \in \mathbb{R}$, is the velocity of the fluid and ν is the kinematic viscosity. Eliminating the pressure p using (2) gives the equation

$$u_t + u \cdot \nabla u = \nu \Delta u + \nabla \{\Delta^{-1}[trace(\nabla u)^2]\}. \tag{3}$$

The turbulence of the fluid is quantified by the dimensionless Reynolds number $R = \frac{UL}{\nu}$ where U is a typical velocity of the flow and L is a typical length scale associated with the flow. The transition to turbulence occurs at $R \sim 500$ and the flow is typically fully turbulent when $R \sim 2000$. Most flows occuring in nature are turbulent even a small stream can have Reynolds number of 10^4 and for a large river it is not unusual that $R \sim 10^6$.

The deterministic Navier-Stokes equation describes laminar flow that may exist when the Reynolds number is large, but then laminar flow is usually unstable. Small noise prevalent in nature is magnified by the instabilities in the flow and it becomes more useful to consider the velocity $u(x,t)$ in turbulent flow to be a stochastic process, see [21]. Then u satisfies a stochastic Navier-Stokes equation

$$\begin{aligned} du &= (\nu\Delta u - u\cdot\nabla u + \nabla\{\Delta^{-1}[trace(\nabla u)^2]\})dt + df_t \\ u(x,0) &= u_0(x). \end{aligned} \tag{4}$$

Here df_t denotes the stochastic forcing in fully developed turbulence.

Much effort has gone into trying to derive the form of the stochastic forcing df_t in the stochastic Navier-Stokes equation (4) for particular cases of fluid flow and flow boundaries. Most of this effort have been in vain because the noise in fully develop turbulence does not seem to care how it arose, at least not sufficiently far away from the boundary. Instead the noise seems to take a general form depending only on that generic small environmental noise was magnified by the fluid instabilities and this growth then saturated by the nonlinearities present in the flow (and in the Navier-Stokes equation), see [11]. The resulting large noise has a generic form. Below we will assume that the stochastic forcing has a general form stipulated by probability theory and use this form and the structure of the Navier-Stokes equation to derive the probability density function (PDF) for turbulence. Then we will compare this PDF with PDFs obtained from simulations and fluid experiments.

If we let D denote the volume in space and put vanishing (or periodic for D a box) velocity boundary condition on the boundary ∂D then we can derive a differential equation relating the mean energy and the mean enstrophy:

$$\mathcal{E} = \frac{1}{2|D|}\int_D |u(x,t)|^2 dx, \quad \Omega = \frac{1}{2|D|}\int_D |\nabla u(x,t)|^2 dx. \tag{5}$$

Here $|D|$ denotes the volume of D and ”mean” refers to the fact that we are dividing the energy and enstrophy by the volume. Multiplying the equation (1) by u and integrating over D we get, by integration by parts,

$$\frac{d}{dt}\mathcal{E} = -2\nu\Omega$$

because all the other terms integrate to zero by the vanishing boundary conditions. The mean energy dissipation is now defined to be

$$\varepsilon = -\frac{d}{dt}\mathcal{E}. \tag{6}$$

3 The Noise in Fully-Developed Turbulence

We will assume that the fluid satisfies periodic boundary conditions on its domain. This is done for convenience and can easily be relaxed. Then the velocity lies in a nice Hilbert space namely $u(x) \in L^2(\mathbb{T}^3)$ or the underlying domain $\mathcal{D}$ can be taken to be a three-torus $\mathbb{T}^3$ and the fluid velocity is in the space of functions square integrable on the torus. By a classical result by Leray [25] one knows that, if $\nabla u(x,0)$ lies in L^2, then $u(x,t)$ lies in L^2 for all t and that one can also make sense of the gradient ∇u for almost every t, at least for the deterministic equation (1).

The stochastic Navier-Stokes equations describing fully developed turbulence is,

$$\begin{aligned} du = (\nu\Delta u - u\cdot\nabla u + \nabla\Delta^{-1}\mathrm{tr}(\nabla u)^2)dt + \sum_{k\in\mathbb{Z}^3} c_k^{\frac{1}{2}} db_t^k e_k(x) \\ + \sum_{k\neq 0} d_k \eta_k dt e_k(x) + u\sum_{k\neq 0}^{m}\int_{\mathbb{R}} h_k \bar{N}^k(dt,dz) \end{aligned} \tag{7}$$

$$u(x,0) = u_0(x)$$

where, in the additive noise, each Fourier component $e_k = e^{2\pi i k\cdot x}$ comes with its own independent Brownian motion b_t^k and a deterministic term $\eta_k t$. The coefficients $c_k^{\frac{1}{2}}$ and d_k decay sufficiently fast so that the Fourier series converges. The sizes of the jumps h_k in the velocity gradient do not decay, but for $t<\infty$, only finitely many $h_k s$, $|k|\leq m$, are nonzero.

The stochastic processes b_t^k are independent. The discrete processes N_t^k are also independent for different ks but can be associated with b_k and $\eta_k t$ for the same k. This link is manifested in the experimentally observed fact that large velocity excursion are accompanied by large dissipation events.

The situation described by the equation (7) is the general situation in turbulent flow. There is some large scale flow that drives all the small scale and one can decompose the velocity field into two parts $U+u$ where U describes the large scale flow and u describes the smaller scale turbulence. In physics u is said to describe the fluctuations. The large scale flow generates a force acting on the small scale and the noise in (7) is a model of this force. We will argue below that based on probability theory this force has a general form in fully developed turbulence. This decomposition of the velocity field can also be thought of as the classical Reynolds decomposition and then the force extерted by the small scales u on the large scales U is the well-known eddy diffusivity. Still another way of thinking about the equation (7) is in terms of the coarse graining of the Navier-Stokes equation, where U describes the mean flow and (7) is the equation describing the fluctuations u.

Turbulent flow consists of complicated and sometimes violent motion that is dissipated in the flow. We split the torus into small boxes and let p_j denote the stochastic dissipation process in the jth box. We assume that the p_js in different boxes are weakly coupled and have mean m. By the Central Limit Theorem [10] in probability theory, the average

$$M_n = \frac{1}{n}\sum_{j=1}^{n} p_j$$

converges to a normal (Gaussian) random variable $\sqrt{n}(M_n - m)/\sigma \to N(0,1)$ as $n \to \infty$, with mean zero and variance one, as we let the number of boxes (n) increase to infinity. We now let

$$S_n = \sum_{j=1}^{n} p_j$$

denote the sum and define the stochastic processes

$$x_t^n = \frac{S_{[tn]} - nm}{\sqrt{n}\sigma}$$

where $[tn]$ denotes integer value. Then if the p_js are independent and identically distributed with variance $\sigma^2 > 0$ and mean m, the functional central limit theorem, see Theorem 8.1 in [9], says that the stochastic processes $\{x_t^n, t \geq 0\}$ converge (in distribution) to a Brownian motion b_t starting at the origin with zero drift and diffusion coefficent 1, as $n \to \infty$. This must be done in the direction of any Fourier component ($e_k = exp(2\pi ik \cdot x)$) that form a basis in the infinite dimensional space L^2 and the result is the differential of an infinite dimensional Brownian motion

$$df_t^1 = \sum_{k \in \mathbb{Z}^3} c_k^{\frac{1}{2}} db_t^k e_k(x).$$

Here each Fourier component comes with its indpendent Brownian motion b_t^k and the $c_k^{1/2}$s are constant vectors.

The Central Limit Theorem says that the average of the dissipation processes converges to a Gaussian but there also exist large excursion or fluctuations in the mean. The effects of these fluctuations are frequently captured by the Large Deviation Principle [39]. If these excursions are completely random then they can, for example, be modeled by a Poisson process with the rate λ. If, moreover, these processes have a bias, an application of the Large Deviation Principle shows that the large deviations of M_n are bounded above by a deterministic term which is a constant determining the direction of the bias, times the rate η. By Theorems 1.3 and 1.5 and Examples 1.3 and 1.5 in [13], since the rate $\lambda_k \to \infty$ as $k \to \infty$ the rate function is bounded by $\eta = \lambda$. This also holds in the direction of each Fourier component and gives the term,

$$df_t^2 = \sum_{k \neq 0} d_k \eta_k dt e_k(x),$$

the second term in the additive noise in stochastic Navier-Stokes equation. Here the d_ks are constant vectors, representing the bias in a particular direction in Fourier space, and the η_k are the rates in the kth direction. We will choose the rate $\eta_k = |k|^{1/3}$ below. This makes the two terms in the additive noise give similar scaling in the Fourier variable k. This must be the case because the second term is capturing the fluctuations in the mean by an application of the Large Deviation Priniciple and thus together the two terms give a more accurate description of the mean. In other words there is only one additive noise term $df_1 + df_2$. It turns out, see below, that the two terms together produce the Kolmogorov-Obukhov '42 scaling. Intermittency in the dissipation is then an additional effect caused by the interaction of the multiplicative and additive noise with the Navier-Stokes evolution. This will be made clear below.

We must also capture the large excursions and intermittency in the velocity and this gives rise to a multiplicative noise term (multiplying the velocity) in the stochastic Navier-Stokes equations. The velocity fluctuations are discrete and if they are completely random they can be modeled by the Poisson jump process x_t^k, with its number process N_t^k denoting the integer number of velocity excursion, associated with kth wavenumber, that have occurred at time t. The differential $dN^k(t) = N^k(t+dt) - N^k(t)$ denotes the number of these excursions in the time interval $(t, t+dt]$. The process

$$\sum_{k \neq 0} \int_{\mathbb{R}} h_k(t,z) \bar{N}^k(dt, dz),$$

in the multiplicative noise, models the excursion (jumps) in the velocity gradient, see [30]. The h_k are the sizes of the jumps in the velocity gradients and $\bar{N}^k$ is the compensated number (of jumps) process. We will include a term in the Poissonian distribution for the jump process that correlates N^k with only the kth Fourier mode. This models the link between large velocity and dissipation events.

The equation (7) represents the stochastic Navier-Stokes equation for the small scales with the general form of turbulent noise. The two terms in the additive noise result from scaling the averge of the dissipation processes in different ways in n (number of processes), but they must both be present, and together they accurately describe the mean dissipation. The coefficents $c_k^{1/2}$ and d_k give their relative size that varies from experiments to experiment, for small k. For large k this ratio should be universal. The Central Limit Theorem and the Large Deviation Principle determine the additive noise in fully developed turbulence, but the multiplicative noise is modeled in (7) as a general (Poisson) jump process. It would also be possible to formulate the equation as the deterministic equation (1) if we continuously modified the initial data so as to absorb the evolving noise. This amounts to continuously modifying the initial data with a stochastic process and is what is effectively done in direct Navier-Stokes simulations (DNS). Clearly, these two formulations must be equivalent.

4 Integral Equation and Spectrum of the Navier-Stokes Operator

We write the stochastic Navier-Stokes equation in integral form,

$$\begin{aligned} u = e^{K(t)} e^{\int_0^t dq} M_t u^0 + \sum_{k \neq 0} c_k^{1/2} \int_0^t e^{K(t-s)} e^{\int_s^t dq} M_{t-s} db_s^k e_k(x) \\ + \sum_{k \neq 0} d_k \int_0^t e^{K(t-s)} e^{\int_s^t dq} M_{t-s} |k|^{1/3} dt \; e_k(x) \end{aligned} \tag{8}$$

where K is the linear (Navier-Stokes) operator

$$K = \nu \Delta + \nabla \Delta^{-1} tr(\nabla u \nabla),$$

$$M_t = exp\{ - \int u(B_s, s) dB_s - \frac{1}{2} \int_0^t |u(B_s, s)| ds \}$$

is a Martingale with $B_t \in \mathbb{R}^3$ an auxiliary Brownian motion, and

$$3\int_s^t dq = \sum_{k\neq 0}^{m} \left\{ \int_0^t \int_{\mathbb{R}} \ln(1+h_k)\bar{N}^k(ds,dz) + \int_0^t \int_{\mathbb{R}} (\ln(1+h_k) - h_k) m_k(ds,dz) \right\},$$

by Ito's formula and a computation similar to the one that produces the geometric Lévy process, see [30]. We have set the rates $\eta_k = |k|^{1/3}$ assuming that the two terms in the additive noise produce similar scalings. The operator K does not generate a semi-group because of its dependence on u but with some conditions on u, see below, it generates a flow. The notation $e^{K(t-s)}f(s)$ simply means that we solve the equation $f_t = Kf$, with initial data $f(s)$ for the time interval $[s,t]$.

The form of the integral equation (8) requires a couple of assumptions. The first observation is that the pressure term $\nabla\Delta^{-1}\mathrm{tr}(\nabla u \cdot \nabla \cdot)$ is independent of the fluid velocity $u(x,t)$ at the point x. This is of course true since x is a set of measure zero and we can be set the integrand to any value at x without changing the integral. In other words the pressure gradient can be treated as a global force that depends on the velocity field as a whole not only on some particular fluid particle. This is consistent with the view of pressure in most of fluid dynamics. The other assumption is that pressure acts as additional diffusion and the integral equation (8) describes a (Ito) diffusion. This is also consistent with most researchers view of pressure but seems to be a more radical assumption from a mathematical point of view. However, it can be proven to be true using the vorticity formulation of the Navier-Stokes equation, see [13]. The first assumption implies that the right hand side of (8) is independent of $u(x,t)$ so that by Ito's formula the integral eqution (8) is equivalent to the initial value problem (7). The second assumption implies that we can apply Girsanov's theorem, see [29], to remove the inertial (drift) term from the operator K above in lieu of the Martingale M_t.

To proceed we need to develop the spectral theory of the operator K. The existence of unique turbulent solutions to the stochastic Navier-Stokes equations (7) can be proven in some cases. For example if the equation is driven by a strong swirling flow, see [12]. This result is not terribly surprising. If the initial data had the symmetry of the swirl then the deterministic problem would be two-dimensional and the global existence of the two-dimensional Navier-Stokes equation is well known. It is also well-known that if the initial data is close to such a two-dimensional flow then global existence can be extened to this case also, see [2, 3], for another such example.

In [12] the author obtained the global bound for the Sobolev space norm of u, based on $L^2(\mathbb{T}^3)$ with index $\frac{11}{6}^+ = \frac{11}{6} + \varepsilon$, ε small, for a swirling flow,

$$E(\|u\|^2_{\frac{11}{6}^+}(t)) \leq C, \tag{9}$$

where E denotes the expectation and the constant C is independent of t. The Sobolev space consists of Hölder continuous functions of Hölder index $1/3$, as pointed out by Onsager [31].

Suppose that

$$E(\|u\|^2_{\frac{3}{2}^+}) \leq C, \tag{10}$$

then the operator K generates a flow denoted by $e^{K(t)}$ and $\lim_{t\to\infty} e^{K(t)} f_0 = 0$, for $f_0 \in H^1(\mathbb{T}^3)$, see [13].

Then using the bound (9) we get an estimate on the operator K.

Lemma 4.1 *Suppose that (9) holds, then the pressure operator is bounded by the spectrum of a symmetric operator with discrete spectrum λ_k^2 and satisfies the estimate*

$$-C|k|^{2/3} \leq -\lambda_k \leq |\nabla\Delta^{-1}\mathrm{tr}\nabla u \cdot \nabla P_k|_2 \leq \lambda_k \leq C|k|^{2/3}, \;\; k \in \mathbb{Z}^3, \tag{11}$$

on the Hilbert space $H^{\frac{11}{6}^+}(\mathbb{T}^3)$, in the inertial range, see below. P_k is the projection onto the kth eigenspace of the symmetric operator. Morover, in the inertial range the operator K satisfies the bound

$$-C|k|^{2/3} + 4\nu\pi^2|k|^2 \leq |KP_k|_2 \leq C|k|^{2/3} - 4\nu\pi^2|k|^2, \;\; k \in \mathbb{Z}^3. \tag{12}$$

We will use this estimate below in order to compute the structure functions of turbulence or the moments of the velocity difference at two points in the fluid, in the inertial range of turbulence, where $1/L \leq |k| \leq 1/\eta$, $k_o = 1/\eta = (\varepsilon/\nu^3)^{1/4}$, a constant. $\eta = 1/k_o$ is called the Kolmogorov length scale, ε is the energy dissipation rate (6) and L is a typical length scale associated with the large eddies in the flow. The above estimate implies that for a large Reynolds number where ν is small and $1/L \leq |k| \leq 1/\eta$, we can think of the spectrum of K growing as a constant times $|k|^{2/3}$, with the error $4\nu\pi^2|k|^2$, in the inertial range, see [13] for more details.

The proof of Lemma 4.1 and the bounds (11) and (12) is the following. A general vector w in $L^2(\mathbb{T}^3)$ can be decomposed into a divergence free and and an irrotational part

$$w = u + v = \nabla \times A + \nabla\phi$$

respectively. The pressure operator $Df = \nabla\Delta^{-1}\mathrm{tr}\nabla u \cdot \nabla f$ maps the subspace U of divergence free vectors in $L^2(\mathbb{T}^3)$ to the subspace of the irrotational vectors V in $L^2(\mathbb{T}^3)$. Thus thus D has no eigenvalues or eigenvectors in U. However, the magnitude of the pressure gradient, the force that keeps the fluid velocity in U, is measure by the norm $|Df|_2$ or by

$$|Df|_2^2 = \langle Df, Df\rangle = \langle f, D^T Df\rangle$$

where D^T is the transpose of D on V. Thus the magnitude of D measured by λ_k where the λ_k^2 are the eigenvalues of the symmetric operator $D^T D$ on the eigenspaces P_k in U, if $D^T D$ has discrete spectrum. We will establish the discreteness of the spectrum and estimate the spectrum of $D^T D$ by comparing it with the spectrum of the symmetric operator $(\partial_x^{2/3})^2$ on U. For $f \in H^{2/3}$, D satisfies the estimate

$$|Df|_2 \leq C\|u\|_{\frac{11}{6}^+}|\partial_x^{2/3} f|_2. \tag{13}$$

The estimate (13) follows from Fourier transform

$$\begin{aligned} \widehat{Df} = \nabla\Delta^{-1}\widehat{\mathrm{tr}\nabla u}\cdot\nabla f &= \frac{2\pi i k}{|k|^2}\mathrm{tr}\sum_{j\neq 0}(k-j)\otimes\hat{u}(k-j)j\otimes\hat{f}(j) \\ &\leq 2\pi\frac{1}{|k|^{3/2}}\mathrm{tr}\sum_{j\neq 0}|k|^{1/2}|j|^{1/3}|k-j||\hat{u}(k-j)||j|^{2/3}|\hat{f}(j)| \\ &\leq \frac{1}{(2\pi)^{3/2}|k|^{3/2^+}}\Big(\sum_{j\neq 0}|\widehat{\partial_x^{\frac{11}{6}^+}u}(k-j)|^2\Big)^{1/2}\Big(\sum_{j\neq 0}|\widehat{\partial_x^{2/3}f}(j)|^2\Big)^{1/2} \end{aligned}$$

by Schwartz's inequality. Now squaring and summing in k we get (13).

Thus for non-degenerate fluid velocities u that satisfy (9), $D^T D$ maps a dense subset of $H^{2/3}(\mathbb{T}^3)\cap U$ onto $L^2(T^3)\cap U$. This means that the resolvent $(I - D^T D)^{-1}$ maps $L^2(\mathbb{T}^3)\cap U$ onto $H^{2/3}(\mathbb{T}^3)\cap U$. Since the latter space sits compactly in the former, $(I - D^T D)^{-1}$ is a compact operator with discrete spectrum. This implies that $D^T D$ also has discrete spectrum.

The estimate (11) follows from the minimax principle, see [19], comparing the eigenvalues of the symmetric operators

$$D^T D \leq C^2\|u\|^2_{\frac{11}{6}^+}(\partial_x^{2/3})^2$$

and taking both branches of the square root. Similarly, (11) follow by comparing the eigenvalues of the symmetric operators

$$(\nu\Delta + D)^T(\nu\Delta + D) = \nu^2\Delta^2 + \nu(D^T\Delta + \Delta D) + D^T D \leq (C\|u\|_{\frac{11}{6}^+}\partial_x^{2/3} + \nu\Delta)^2.$$

This concludes the proof of Lemma 4.1, [13] can be consulted for more details.

5 The Log-Poissonian Processes

The processes found by She and Leveque [35], and shown to be log-Poisson processes by She and Waymire [36] and by Dubrulle [16], are produced by applying the Feynmann-Kac formula to the potential dq. Namely, $e^{\int_0^t dq} = e^{\sum_{k\neq 0}^m \int_0^t dq_k}$ and by setting $h_k = \beta - 1$ and computing the mean of N_t^k

$$E(N_t^k) = \int_{\mathbb{R}} m_k(t,dz) = -\frac{\gamma \ln|k|}{\beta - 1}, \tag{14}$$

we get that

$$\begin{aligned} 3\int_0^t dq_k &= \int_0^t \int_{\mathbb{R}} \ln(1+h_k)\bar{N}^k(ds,dz) + \int_0^t \int_{\mathbb{R}} (\ln(1+h_k) - h_k) m_k(ds,dz) \\ &= N_k(t)\ln(\beta) + (\beta - 1)(\gamma \frac{\ln|k|}{\beta - 1}), \end{aligned}$$

so we get the term

$$e^{\int_0^t dq_k} = e^{(\gamma \ln|k| + N_k \ln \beta)/3} = \left(|k|^\gamma \beta^{N_k}\right)^{1/3} = \left(|k|^\gamma \beta^{N_t^k}\right)^{1/3} \tag{15}$$

in the (implicit) solution (8) of the stochastic Navier-Stokes equation. These are exactly the log-Poisson processes found by the above authors. This gives

$$\ln E((e^{\gamma \ln|k| + N_k \ln \beta})^{\frac{p}{3}}) = \ln E((|k|^\gamma \beta^{N_k})^{\frac{p}{3}}) = \gamma(\frac{p}{3} - \frac{\beta^{p/3} - 1}{\beta - 1}) \ln|k| = -\tau_p \ln|k|,$$

for the logarithm of the pth moment, where τ_p are the intermittency corrections in (20). Now the expression

$$\tau_p = -\gamma(\frac{p}{3} - \frac{\beta^{p/3} - 1}{\beta - 1})$$

implies that $\tau_0 = 0$ and $\tau_3 = 0$ independently of γ. The latter condition is required by the Kolmogorov 4/5th law, see [17]. However, to be consistent with the spectral theory of the operator D above that moves energy around in quanta of $|k|^{2/3}$ we should set $\gamma = 2/3$. This means that the log-Poissionian processes also move energy in quanta of $|k|^{2/3}$ in Fourier space. However, $|k|^{2/3}$ is multiplied by $\beta^{N_t^k}$ in (15) above, namely the number of jumps on the kth level contribute to the transfer of energy, and so far β is a free parameter. We follow [35] in making the assumption that determines β, see also [37]. The basic assumption is that the most singular structures in the turbulent fluid are one-dimensional vortex lines that the highest moments capture. Thus (assuming $0 < \beta < 1$) by the Lagrange transformation, see [35],

$$\tau_p = -\frac{2}{3}\left(\frac{p}{3}\right) + \frac{2}{3}\frac{1}{1-\beta} - \frac{2}{3}\frac{\beta^{p/3}}{1-\beta} \to -\frac{2}{3}\left(\frac{p}{3}\right) + \frac{2}{3}\frac{1}{1-\beta} = -\frac{2}{3}\left(\frac{p}{3}\right) + C_o$$

as $p \to \infty$, where $C_o = 2$ is the codimension of the one-dimensional vortex lines and this implies that $\beta = 2/3$. We will make this choice of β.

Thus we see that the jumps multiplying u in the equation (7) produce the log-Poisson processes $(|k|^{\frac{2}{3}}\left(\frac{2}{3}\right)^{N_t^k})^{\frac{1}{3}}$ in the integral equation for u.

$$\begin{aligned} u &= e^{K(t)}(\prod_k^m |k|^{\frac{2}{3}}(2/3)^{N_t^k})^{\frac{1}{3}} M_t u_0 \\ &+ \sum_{k\neq 0} c_k^{1/2} \int_0^t e^{K(t-s)}(\prod_j^m |j|^{\frac{2}{3}}(2/3)^{N_{(t-s)}^j}) M_{t-s} db_s^k e_k(x) \\ &+ \sum_{k\neq 0} d_k \int_0^t e^{K(t-s)}(\prod_j^m |j|^{\frac{2}{3}}(2/3)^{N_{(t-s)}^j})^{\frac{1}{3}} M_{t-s}|k|^{1/3} dt\ e_k(x) \end{aligned}$$

since only the kth log-Poissonian processes are correlated with the kth Fourier component. This equation clearly shows how the intermittency in the velocity (in Equation (7)) causes intermittency in the dissipation through the Navier-Stokes evolution, if we recall how the discrete (Poisson) distribution picks the kth term (associated with e_k) out of the product.

6 The Kolmogorov-Obukhov-She-Leveque Theory

In 1941 Kolmogorov and Obukhov [21, 20, 27] proposed a statistical theory of turbulence based on dimensional arguments. The main consequence and test of this theory was that the structure functions of the velocity differences of a turbulent fluid

$$E(|u(x,t) - u(x+l,t)|^p) = S_p = C_p l^{p/3}$$

should scale with the distance (lag variable) l between them, to the power $p/3$. This theory was immediately criticized by Landau for not taking into account the influence of the large flow structure on the constants C_p and later for not including the influence of the intermittency in the velocity fluctuations on the scaling exponents, see [1].

In 1962 Kolmogorov and Obukhov [22, 28] proposed a corrected theory were both of the above issues were addressed. They presented their refined similarity hypothesis

$$S_p = C'_p < \tilde{\varepsilon}^{p/3} > l^{p/3} \tag{16}$$

where l is the lag variable and the averaged energy dissipation rate is

$$\tilde{\varepsilon} = \frac{1}{\frac{4}{3}\pi l^3} \int_{|s|\leq l} \varepsilon(x+s)ds \tag{17}$$

ε being the mean energy dissipation rate (6). They also pointed out that the scaling exponents for the first two structure functions could be corrected by log-normal processes. However, for higher order structure functions the log-normal processes gave intermittency corrections inconsistent with contemporary simulations and experiments.

In the refined similarity hypothesis (16) the averaged dissipation rate $\tilde{\varepsilon}$ will depend on the large flow structure, so its addition addresses Landau's objections at least partially. The assumption is that

$$< \tilde{\varepsilon}^{p/3} > \sim l^{\tau_p},$$

because of intermittency, where the τ_p are called the intermittency corrections (to the scaling). Consequently, intermittency corrections are also produced,

$$S_p = C'_p < \tilde{\varepsilon}^{p/3} > l^{p/3} = C_p l^{p/3+\tau_p} = C_p l^{\zeta_p},$$

where the

$$\zeta_p = \frac{p}{3} + \tau_p$$

are the scaling exponents with intermittency corrections included and the C_p are not universal but depend on the large flow structure. We will see below that starting with (7) this scaling hypothesis in fact holds.

The She-Leveque intermittency corrections are

$$\tau_p = -\frac{2p}{9} + 2(1-(2/3)^{p/3})$$

given by the log-Poissonian processes derived above. These intermittency corrections are consistent with contemporary simulations and experiments, see [1], [34], [35] and [37].

7 Estimates of the Structure Functions

We will now show how the integral form (8) can be used to compute an estimate for the structure functions of turbulence.

In order to compute the structure functions of turbulence or the moments of the velocity difference at two points in the fluid, we need to estimate the the operator K above, compare Equation (11). Recall the eigenvalues $\lambda_k > 0$ that are the square roots of the eigenvalues of the symmetric operator $D^T D$ above, with P_k the projector onto the corresponding eigenspace. Then the equation (12) can be reformulated as

$$\begin{aligned} -C|k|^{2/3} + 4\nu\pi^2|k|^2 \leq -\lambda_k + \nu 4\pi^2|k|^2 &\leq |KP_k|_2 \\ &\leq \lambda_k - \nu 4\pi^2|k|^2 \leq C|k|^{2/3} - \nu 4\pi^2|k|^2, \end{aligned} \tag{18}$$

if u satisfies the bound

$$E(\|u\|_{\frac{11}{6}+})(t) \leq C, \tag{19}$$

by the above. For a large Reynolds number ν is small and since $|k|^2 \leq k_o^2$, $k_o = (\varepsilon/\nu^3)^{1/4}$, where k_0 is the inverse of the Kolmogorov length, we can now think of the spectrum of K growing as a constant times $|k|^{2/3}$ in the inertial range. ε is the dissipation rate (6). The coefficient C is a constant times a Sobolov space norm of u, by the estimate (13), see [12].

Now estimates of the structure function are possible and we get the following result. Suppose that the coefficients c_k and d_k in equation (4) satisfy the conditions $\sum_{k\in\mathbb{Z}^3} c_k < \infty$ and $\sum_{k\in\mathbb{Z}^3\setminus\{0\}} |k|^{1/3}|d_k| < \infty$. Then the scaling of the structure functions of (4) is

$$S_p \sim C_p|x-y|^{\zeta_p}, \tag{20}$$

where

$$\zeta_p = \frac{p}{3} + \tau_p = \frac{p}{9} + 2(1-(2/3)^{p/3}) \tag{21}$$

$\frac{p}{3}$ being the Kolmogorov-Obukhov '41 scaling and τ_p the She-Leveque intermittency corrections, when the lag variable $|x-y|$ is small.

The values in equation (21) agree with experimental values in [34], they are in agreement with Kolmogorov-Obukhov scaling hypothesis with intermittency corrections, computed by She and Leveque, but disagree with the log-normal distribution [22, 28], for the intermittency corrections.

The estimate of the first structure function is straight-forward,

$$
\begin{aligned}
& S_1(x,y,t) = E(|u(x,t)-u(y,t)|) = \\
& 2\sum_{k\in\mathbb{Z}^3\backslash\{0\}} d_k \int_0^t e^{-\lambda_k(t-s)}|k|^{1/3}ds\, E([e^{\gamma\ln|k|+N_k\ln(\beta)}]^{1/3})\sin(\pi k\cdot(x-y)) \\
(22) \quad & \leq \frac{2}{C}\sum_{k\in\mathbb{Z}^3\backslash\{0\}} |d_k|\frac{(1-e^{-\lambda_k t})}{|k|^{\zeta_1}}|\sin(\pi k\cdot(x-y))|.
\end{aligned}
$$

We have estimated $K(t)$ by $\lambda_k \approx C|k|^{2/3}$ in the second line (we use this approximation throughout the computations) and also used the expectation of the Poisson jump process

$$
E([e^{\gamma\ln|k|+N_k\ln(\beta)}]^{1/3}) = \frac{1}{|k|^{\tau_1}}.
$$

We used the lower estimate in (18) and this makes the estimate in (22) be an overestimate. The measure of the discrete process must be written as

$$
\sum_{l=-\infty}^{\infty}\delta_{l,k}\prod_{j\neq l}^{m}\delta_{N_t^j}\sum_{j=0}^{\infty}(\cdot)\frac{m_l^j}{j!}e^{(-m_l)}, \tag{23}
$$

where $\delta_{l,k} = 0, l\neq k, 1, l = k$ is the Kronecker delta function, because N_t^k depends on the kth Fourier component e_k (or db_t^k and $|k|^{1/3}dt$) but is independent of the components with different wavenumbers. The δ functions in the product imply that the probabilities of all the N_t^js, $j\neq k$ consentrate at 0.

Now, if $\sum_{k\in\mathbb{Z}^3\backslash\{0\}}|d_k| < \infty$, then we get a stationary state as $t\to\infty$

$$
S_1(x,y,\infty) \leq \frac{2}{C}\sum_{k\in\mathbb{Z}^3\backslash\{0\}}\frac{|d_k|}{|k|^{\zeta_1}}|\sin(\pi k\cdot(x-y))|
$$

and for $|x-y|$ small,

$$
S_1(x,y,\infty) \sim \frac{2\pi^{\zeta_1}}{C}\sum_{k\in\mathbb{Z}^3\backslash\{0\}}|d_k||x-y|^{\zeta_1},
$$

where $\zeta_1 = 1/3+\tau_1 \approx 0.37$.

A similar computation gives the second structure function,

$$\begin{aligned} S_2 &= E(|u(x,t)-u(y,t)|^2) \\ &\le \frac{2}{C}\sum_{k\in\mathbb{Z}^3\setminus\{0\}} c_k \frac{1-e^{-2\lambda_k t}}{|k|^{\zeta_2}}\sin^2(\pi k\cdot(x-y)) \\ &+ \frac{4}{C^2}\sum_{k\in\mathbb{Z}^3\setminus\{0\}} {d_k}^2 \frac{(1-e^{-\lambda_k t})^2}{|k|^{\zeta_2}}\sin^2(\pi k\cdot(x-y)), \end{aligned}$$

again by using the lower estimate in (18). As $t\to\infty$, we get

$$S_2(x,y,\infty)\sim\frac{4\pi^{\zeta_2}}{C^2}\sum_{k\in\mathbb{Z}^3\setminus\{0\}}[{d_k}^2+(\frac{C}{2})c_k]|x-y|^{\zeta_2},$$

when $|x-y|$ is small, where $\zeta_2 = 2/3+\tau_2\approx 0.696$.

Similarly

$$\begin{aligned} S_3 &= E(|u(x,t)-u(y,t)|^3) \\ &\le \frac{2^3}{C^3}\sum_{k\in\mathbb{Z}^3\setminus\{0\}}\frac{[|d_k|^3(1-e^{-\lambda_k t})^3+3(C/2)c_k|d_k|(1-e^{-2\lambda_k t})(1-e^{-\lambda_k t})]}{|k|} \\ &\times |\sin^3(\pi k\cdot(x-y))|, \end{aligned}$$

and

$$S_3(x,y,\infty)\sim\frac{2^3\pi}{C^3}\sum_{k\in\mathbb{Z}^3\setminus\{0\}}[|d_k|^3+3(C/2)c_k|d_k|]|x-y|.$$

All the structure functions are computed in a similar manner, for the pth structure functions, we get that S_p is estimated by

$$S_p\le\frac{2^p}{C^p}\sum_{k\in\mathbb{Z}^3\setminus\{0\}}\frac{\sigma^p\cdot(-i\sqrt{2}M)^p\, U\left(-\frac{1}{2}p,\frac{1}{2},-\frac{1}{2}(M/\sigma)^2\right)}{|k|^{\zeta_p}}|\sin^p(\pi k\cdot(x-y))|.$$

where U is the confluent hypergeometric function, $M=|d_k|(1-e^{-\lambda_k t})$ and $\sigma=\sqrt{(C/2)c_k(1-e^{-2\lambda_k t})}$. Thus the coefficients of S_p are given by the raw moments of a Gaussian, the first few of which are listed in Table 1. Now $S_p(x,y,\infty)$ is

$$S_p\sim\frac{2^p\pi^{\zeta_p}}{C^p}\sum_{k\in\mathbb{Z}^3\setminus\{0\}}((C/2)c_k)^{p/2}\cdot(-i\sqrt{2}|d_k|)^p\, U\left(-\frac{1}{2}p,\frac{1}{2},-\frac{d_k^2}{Cc_k}\right)|x-y|^{\zeta_p},$$

Table 1: Moments of a Gaussian

Order	Raw moment	Central moment	Cumulant
1	M	0	M
2	$M^2 + \sigma^2$	σ^2	σ^2
3	$M^3 + 3M\sigma^2$	0	0
4	$M^4 + 6M^2\sigma^2 + 3\sigma^4$	$3\sigma^4$	0
5	$M^5 + 10M^3\sigma^2 + 15M\sigma^4$	0	0
6	$M^6 + 15M^4\sigma^2 + 45M^2\sigma^4 + 15\sigma^6$	$15\sigma^6$	0
7	$M^7 + 21M^5\sigma^2 + 105M^3\sigma^4 + 105M\sigma^6$	0	0
8	$M^8 + 28M^6\sigma^2 + 210M^4\sigma^4 + 420M^2\sigma^6 + 105\,\sigma^8$	$105\sigma^8$	0

to leading order for $|x-y|$ small. We also obtain Kolmogorov's $4/5$ law, see [17],

$$S_3 = -\frac{4}{5}\varepsilon(0)|x-y|$$

to leading order, were ε is the mean energy dissipation rate (6).

8 The Invariant Measure of Turbulence

The invariant measure of the stochastic Navier-Stokes equation determines all the one-point statistics of turbulence, or the statistics of quantities defined at one point x in the flow. This quantity determines all the statistical properties of the turbulent velocity field, see [33], and in distinction to the nonlinear Navier-Stokes equation, the invariant measure satisfies a linear but a functional differential equation, see [33]. In fact Hopf [18] found a linear equation for the characteristic function (Fourier transform) of the invariant measure in 1952, but at that time methods for solving such an equation were not available. In Hopf's equation the noise for fully developed turbulence was missing, but in Kolmogorov's equation for the invariant measure the noise is always supplied. Since only the linearized Navier-Stokes equation appears in the Kolmogorov-Hopf equation, below, for the invariant measure, we will think about the linearized Navier-Stokes equation as the infinite-dimensional Ito process whose generator gives the Kolmogorov-Hopf equation.

Thus associated with such an Ito process is a diffusion equations, a linear functional differential equation that is the Kolmogorov-Hopf equation determining the invariant measure. We will now derive this equation. This will make clear how to compute the coefficients in the Kolmogorov-Hopf equation.

The Kolmogorov-Hopf equation for the invariant measure is

$$\frac{\partial\phi}{\partial t} = \frac{1}{2}\mathrm{tr}[P_t C P_t^* \Delta\phi] + \mathrm{tr}[P_t \bar{D}\nabla\phi] + < \bar{K}(z)P_t, \nabla\phi >, \tag{24}$$

where $\bar{D} = (|k|^{1/3}d_k)$, $\phi(z)$ is a bounded function of z and $|x| =< x,x >^{1/2}$ where $< \cdot,\cdot >$ is the inner product on H. Here $C^{1/2}$, $D \in L(H)$ are linear operators on $H = L^2(\mathbb{T}^3)$, defined by

$$C^{1/2}u = \sum_{k\neq 0} C_k^{\frac{1}{2}} \hat{u}_k e_k, \; Du = \sum_{k\neq 0} D_k \hat{u}_k e_k$$

for $u = \sum_{k\neq 0} \hat{u}_k e_k \in L^2(\mathbb{T}^3)$, $C_k^{1/2}$ and D_k are 3 by 3 diagonal matricies with entries $c_{k,j}^{1/2}$ and $d_{k,j}$, $j = 1,2,3$ on the diagonal.

$$P_t = e^{-\int_0^t \nabla u \, dr} \prod_k^m (|k|^{2/3}(2/3)^{N_t^k})^{\frac{1}{3}},$$

by the computation of how the log-Poisson processes are produced, from the Navier-Stokes equation, by the Feynmann-Kac formula (15) above. The operator $\bar{K}$ is the linearized Navier-Stokes operator

$$\bar{K} = \nu\Delta - u\cdot\nabla + 2\nabla\Delta^{-1}tr(\nabla u \nabla) = K - u\cdot\nabla.$$

and z is the solution of the linearized Navier-Stokes equation. Notice that now K has a 2 in front of the pressure term as in Section 7.

To find the infinite-dimensional Ito process whose Kolmogrov's backward equation is (24), we consider the linearized Navier-Stokes equation with the same noise as (7), see Section 7. This is the functional derivative of the deterministic Navier-Stokes equation (1), driven with the same noise as the stochastic equation (7), to give an Ito process in function space. It is analogous to the stochastic evolution of the volume element in finite dimensions, but here the Ito process determines the evolution of any bounded function of u, in infinite dimensions, see [33]. The solution of the linearized Navier-Stokes equation can be written in integral form as

$$z = e^{Kt}P_tM_tz^0 + \sum_{k\neq 0} c_k^{1/2}\int_0^t e^{K(t-s)}P_{t-s}M_{t-s}db_s^k e_k(x)$$

$$+\sum_{k\neq 0} d_k \int_0^t e^{K(t-s)}P_{t-s}M_{t-s}|k|^{1/3}ds\, e_k(x) \tag{25}$$

by the Feynmann-Kac formula, where is the operator K generates the flow e^{Kt}, and

$$M_t = exp\{-\int u(B_s,s)dB_s - \frac{1}{2}\int_0^t |u(B_s,s)|ds\}$$

is a Martingale with $B_t \in \mathbb{R}^3$ an auxiliary Browninan motion, see Section 7.

Now we define the variance

$$Q_t = \int_0^t e^{K(s)}P_sM_sCM_sP_s^* e^{K^*(s)}ds \tag{26}$$

and drift

$$E_t = \int_0^t e^{K(s)}P_sM_s\bar{D}ds \tag{27}$$

operators. Then the solution of the Kolmogorov-Hopf equation (24) can be written in the form

$$R_t\phi(z) = \int_H \phi(y)\mathcal{N}_{(e^{Kt}P_tM_tz+E_tI,Q_t)} * \mathbb{P}_{P_t}(dy)$$
$$= \int_H \phi(e^{Kt}P_tM_tz + E_tI + y)\mathcal{N}_{(0,Q_t)} * \mathbb{P}_{P_t}(dy)$$

where $\mathbb{P}_{P_t}$ is the Poisson law of P_t, see [33]. $\mathcal{N}_{m,Q_t}$ denotes the infinite-dimensional normal distribution on H with mean m and variance Q_t, $I = \sum e_k, E_tI \in H$.

8.1 The Invariant Measure of Turbulence

We can now write a formula for the invariant measure of turbulence.

Theorem 8.1 *The invariant measure of the stochastic Navier-Stokes equation on $H_c = H^{3/2^+}(\mathbb{T}^3)$ has form*

$$\mu(dx) = e^{<Q^{-1/2}EI,\, Q^{-1/2}x>-\frac{1}{2}|Q^{-1/2}EI|^2}\mathcal{N}_{(0,Q)}(dx)\sum_k \delta_{k,l}\prod_{j\neq l}^m \delta_{N_t^j}\sum_{j=0}^\infty p_{m_l}^j\delta_{(N_t^l-j)} \tag{28}$$

where $Q = Q_\infty$, $E = E_\infty$, $m_k = \ln|k|^{2/3}$ is the mean of the log-Poisson processes (14) and $p^j_{m_k} = \frac{(m_k)^j e^{-m_k}}{j!}$ is the the probability of $N^k_\infty = N_k$ having exactly j jumps, $\delta_{k,l}$ is the Kroncker delta function.

Suppose that the operator Q is trace-class, $E(Q^{1/2}H) \subset Q^{1/2}(H)$ and that $e^{Kt}P_tM_t(H) \subset Q_t^{1/2}(H),\ t > 0$, where $H = H_c$, then, with u given, the invariant measure μ is unique, ergodic and strongly mixing. We know that the above invariant measure is unique for the strong swirl [12] and strong rotation [2, 3] but it depends on u, and its uniqueness for general turbulent flows depends on the uniqueness of u.

The proof of Theorem 8.1 uses the above machinery and is analogous to the proof of Theorem 8.20 in [33], see [13] for details.

9 The Invariant Measure for the Velocity Differences

We will now find the Kolmogorov-Hopf functional differential equation for the invariant measure of the Navier-Stokes equation for the velocity differences

$$z = u - w = u(x,t) - u(y,t).$$

The previous measure was the measure determining the 1-point statistics but the measure for the velocity difference will determine the 2-point statistics. We are simplifying this a little using isotrophy; namely, in general the velocity difference is a tensor. The linearized Navier-Stokes operator is now

$$\bar{K} = \nu\Delta - u\cdot\nabla + \nabla\Delta^{-1}tr((\nabla u + \nabla w)\nabla),$$

but otherwise the derivation is similar to the derivation of the $1-$point measure above. The formula for the $2-$point measure is the same (28), but now the operator K depends on the two points x and y and therefore the variance (26) and the drift (27), will also depend on these two points. In fact the measure depends on the lag variable $x-y$. A better way of capturing the dependence on the lag variable is to write the difference of the inertial terms as

$$-u\cdot\nabla w + w\cdot\nabla u = -u\cdot\nabla(u-w) - (u-w)\cdot\nabla u + (u-w)\cdot\nabla(u-w)$$

This produces the new operator

$$\tilde{K} = \nu\Delta - u\cdot\nabla + z\cdot\nabla - \nabla u + \nabla\Delta^{-1}tr((\nabla u + \nabla w)\nabla) = K - u\cdot\nabla + z\cdot\nabla - \nabla u$$

with the understanding that now K is a function of $(\frac{(u+w)}{2})$ through the pressure term. The last three terms are removed by a combination of Feynmann-Kac and the Cameron-Martin formula (Girsanov's theorem) and we get the martingale

$$M_t = exp\{\int_0^t u(x - B_{-s} + y, s) \cdot dB_{-s} + \int_0^t z(B_s) \cdot dB_s - \frac{1}{2}\int_0^t |u(x - B_{-s} + y, s) + z(B_s), s)|^2 ds\}$$

after a time reversal of the auxiliary Brownian motion B_t see [26]. The computation of the measure follows the procedure for the computation of the measure for the 1-point statistics. The difference of the two equations (for u and w) is written as an integral equation

$$\begin{aligned} z &= e^{K(t)} e^{-\int_0^t \nabla u \, ds} e^{\int_0^t dq} M_t z^0 + \sum_{k \neq 0} c_k^{1/2} \int_0^t e^{K(t-s)} e^{-\int_s^t \nabla u \, dr} e^{\int_s^t dq} M_{t-s} db_s^k e_k(x) \\ &+ \sum_{k \neq 0} d_k \int_0^t e^{K(t-s)} e^{-\int_s^t \nabla u \, dr} e^{\int_s^t dq} M_{t-s} |k|^{1/3} ds \, e_k(x) \end{aligned} \tag{29}$$

by the Feynmann-Kac formula and Girsanov's theorem where K is the operator

$$K = \nu\Delta + \nabla\Delta^{-1} tr((\nabla u + \nabla w)\nabla), \tag{30}$$

and

$$P_t = e^{-\int_0^t \nabla u \, ds} e^{\int_0^t dq} M_t = e^{-\int_0^t \nabla u \, dr} \prod_k |k|^{2/3} (2/3)^{N_t^k} M_t.$$

The Kolmogorov-Hopf equation for the Ito processes (29) now becomes

$$\frac{\partial \phi}{\partial t} = \frac{1}{2} \text{tr}[P_t C P_t^* \Delta \phi] + \text{tr}[P_t \bar{D} \nabla \phi] + < K(z) P_t, \nabla \phi >, \tag{31}$$

where $\bar{D} = (|k|^{1/3} D_k)$ and $\phi(z)$ is a bounded function of z. It is also the Kolmogorov backward equation of the Ito process (29).

The variance is

$$Q_t = \int_0^t e^{K(s)} P_s C P_s^* e^{K^*(s)} ds \tag{32}$$

and the drift is

$$E_t = \int_0^t e^{K(s)} P_s \bar{D} ds. \tag{33}$$

Then the solution of the Kolmogorov-Hopf equation (31) can be written in the form

$$R_t\phi(z) = \int_H \phi(y)\mathcal{N}_{(e^{K(t)}P_t z+E_t I,Q_t)} * \mathcal{N}_{(0,2\nu)} * \mathbb{P}_{P_t}(dy)$$
$$= \int_H \phi(e^{K(t)}P_t z+E_t I+y)\mathcal{N}_{(0,Q_t)} * \mathcal{N}_{(0,2\nu)} * \mathbb{P}_{P_t}(dy) \tag{34}$$

where $\mathbb{P}_{P_t}$ is the Poisson law of P_t, see [33]. Here $|x| = < x,x >^{1/2}$ where $< \cdot,\cdot >$ is the inner product on H, and $z = z_0$. $\mathcal{N}_{m,Q_t}$ denotes the infinite-dimensional normal distribution on H with mean m and variance Q_t, $I = \sum e_k, E_t I \in H$ and $\mathcal{N}_{(0,2\nu)}$ the the law of the three-dimensional Brownian motion in the Martingale M_t. If Q_t is of trace-class $Q_t \in L^+(H)$, then R_t is Markovian.

Theorem 9.1 *The invariant measure for the velocity differences (two-point statistics) of the Navier-Stokes equation on $H_c = H^{3/2^+}(\mathbb{T}^3)$ has form*

$$\mu(dx,dy) = e^{<Q^{-1/2}EI,\ Q^{-1/2}x> - \frac{1}{2}|Q^{-1/2}EI|^2}\mathcal{N}_{(0,Q)}(dx) * \mathcal{N}_{(0,2\nu)}(dy)\sum_k \delta_{k,l}\sum_{j=0}^{\infty} p^j_{m_l}\delta_{(N_l-j)} \tag{35}$$

where $Q = Q_\infty$, $E = E_\infty$. Here $m_k = \ln|k|^{2/3}$ is the mean of the log-Poisson processes (14) and $p^j_{m_k} = \frac{(m_k)^j e^{-m_k}}{j!}$ is the the probability of $N^k_\infty = N_k$ having exactly j jumps, $\delta_{k,l}$ is the Kroncker delta function.

Suppose that the operator Q is trace-class, $E(Q^{1/2}H) \subset Q^{1/2}(H)$ and that

$$e^{K(t)}P_t(H) \subset Q_t^{1/2}(H),\ t > 0,$$

where $H = L^2(\mathbb{T}^3)$, then, given u, the invariant measure μ is unique, ergodic and strongly mixing. The proof of Theorem 9.1 is similar to the proof of Theorem 8.1, see [13] for details.

It is easy to check that the moments of the invariant measure for the two-point statistics give the estimates for the structure functions above. The variable in the latter three-dimensional Gaussian $\mathcal{N}_{(0,2\nu)}(dy)$ in the invariant measure is the lag variable.

The same comments as above apply to the measure (35) as the invariant measure for the one-point statistics (28). It is unique for the strong swirl [12] and strong rotation [2, 3] but its uniqueness for general turbulent flows depends on the uniqueness of u.

10 The Differential Equation for the PDF

We must compute the PDF of the invariant measure (28), for the velocity differences, in order to compare with PDFs constructed from simulations and experiments. The simplest way of doing this is to derive the differential equation for the density function from the Kolmogorov-Hopf equation (24). We start by rewriting the equation Kolmogorov-Hopf (24) in the form

$$\frac{\partial \phi}{\partial t} = \frac{1}{2}\mathrm{tr}[Q_t \Delta \phi] + \mathrm{tr}[E_t \nabla \phi] \tag{36}$$

where Q_t and E_t are respectively time-derivatives of the variance (26) and drift (27), but computed with the operator K in (30). This can be done by redefining the underlying infinite-dimensional Ito process appropriety, see [13]. We have to take the trace of the functional variables to get the equation for the PDF. The resulting equation is

$$\frac{\partial \phi}{\partial t} = \frac{1}{2}\Delta \phi + \frac{1}{\sqrt{2t}} c \cdot \nabla \phi \tag{37}$$

where $\hat{c}(|k|) = (Q_t^{-1/2} E_t)_k$ are coefficients, after we scale by the variance Q_t. Now scaling the equation by $-2t$ and sending $t \to \infty$ gives the equation

$$\frac{1}{2}\Delta \phi + c \cdot \nabla \phi = \phi. \tag{38}$$

with a trivial rescaling of time. This is the (stationary) equation for the distribution function. Now the PDF is for the absolute value of the velocity differences $w = |u(x,t) - u(y,t)|$, by the Equation (43) below, so the angle derivatives of w do not appear, and $\hat{c} = (Q^{-1/2}E)_k \sim \bar{c}|k|^{1/3}/|k|^{1/3} = \bar{c}$ for k large. Thus, taking the trace of the spatial (lag) variables also, we get that $c = \frac{\bar{c}}{w}$. In polar cordinates $\Delta \phi = \phi_{ww} + \frac{2}{w}\phi_w$, in three dimensions. Thus (38) becomes

$$\frac{1}{2}\phi_{ww} + \frac{1+\bar{c}}{w}\phi_w = \phi. \tag{39}$$

This is the stationary equation satisfied by the PDF.

The above computation is clarified by the following example. Consider the equation

$$\phi_t = \phi_{xx} + \frac{c}{\sqrt{2t}}\phi_x$$

where $\phi = \frac{e^{-(x-a)^2/b}}{\sqrt{\pi b}}$ is a Gaussian. It is easy to check that this equation holds if $a_t = -\frac{c}{\sqrt{2t}}$ and $b_t = 4$, so $a = -c\sqrt{2t}$ and $b = 4t$. Thus invariant measure is produced by scaling out t,

$$\phi(y)dy = \frac{e^{-\frac{(y+c)^2}{2}}}{\sqrt{2\pi}}dy = \frac{e^{\frac{(y-\frac{a}{\sqrt{b/2}})^2}{2}}}{\sqrt{2\pi}}dy = \phi(x,t)dx.$$

where $y = x/\sqrt{2t}$. This invariant measure satisfies the stationary equation (38).

11 The PDF for the Turbulent Velocity Differences

It is now possible to compute the probability density function (PDF) for the velocity differences in turbulence, knowing the asymptotics of the structure functions.

The form of the equation (39) suggests that we should look for a solution of the form $f = x^a K_\lambda$ where K_λ is a modified Bessel's function of the second kind, satisfying the equation,

$$K_{xx} + \frac{1}{x}K_x - (1 + \frac{\lambda^2}{x^2})K = 0.$$

A substitution of this ansatz into the equation (39) gives $a = -\bar{c}$ and $\lambda = \sqrt{\frac{\bar{c}(\bar{c}+1)}{2}}$. The solution is the generalized hyperbolic distribution, see Barndorff-Nilsen [4]. It has an algebraic cusp at the origin and exponential tails and is constructed by multiplying the modified Bessel's function of the second kind K_λ, by $x^{-\lambda}$. For the zeroth moment we get a distinguished solution $\lambda = \bar{c} = 1$ which give the Normal Inverse Gaussian (NIG) distribution that was also investigated by Barndorff-Nilsen [5] and used by Barndorff-Nilsen, Blæsild and Schmiegel to model PDF of velocity increments for several data sets in [7]. It turns out that the distribution functions for all of the moments can be expressed by the NIG distribution function. However, since the intermittence corrections are different for the different moments the NIG distributions for the different moments have different parameters, as will be explained below.

The PDF of the NIG is

$$\frac{\alpha\delta K_1\left(\alpha\sqrt{\delta^2 + (x-\mu)^2}\right)}{\pi\sqrt{\delta^2 + (x-\mu)^2}}\, e^{\delta\gamma + \beta(x-\mu)} \tag{40}$$

The parameters are:

$$\alpha \quad \text{heavyness of the tail}, \; \beta \quad \text{asymmetry}, \; \delta \quad \text{scaling}$$
$$\mu \quad \text{centering}, \; \gamma = \sqrt{\alpha^2 - \beta^2}.$$

The NIG distribution has very nice properties that are summarized in [7]. In particular its characteristic function and all of its moments are easily computed. However, the moments of the velocity differences are not the moments of the same NIG distributions because of the intermittency correction. In fact, the invariant measure (35) has both a continuous and a discrete part and because of this each moment comes with its own PDF, as mentioned above. All of these PDF are solutions of the stationary equation (39) and they can be expressed in terms of NIG distributions. However, their parameters α, β, δ and μ all depend on the particular moment for which one is computing the PDF. Thus these parameters are different for the different moments. The cumulant generating function $\mu z + \delta(\gamma - \sqrt{\alpha^2 - (\beta + z)^2})$ is particularly simple for the NIG and this make the moments easy to compute, see [7]. The first few moments and the characteristic function of the NIG distribution are:

$$(41) \qquad \begin{array}{cl} \text{Mean} & \mu + \delta\beta/\gamma \\ \text{Variance} & \delta\alpha^2/\gamma^3 \\ \text{Skewness} & 3\beta/(\alpha\sqrt{\delta\gamma}) \\ \text{Excess kurtosis or flatness} & 3(1 + 4\beta^2/\alpha^2)/(\delta\gamma) \\ \text{Characteristic Function} & e^{i\mu z + \delta(\gamma - \sqrt{\alpha^2 - (\beta + iz)^2})} \end{array}$$

However, since the parameters α, β, δ and μ are different for different moments, care must be taken when the moments above are used the compute these parameters. This will be discussed in more details in the next section.

Thus we see that the probability density function of the velocity increment is a normalized inverse Gaussian (NIG) distribution that is a generalized hyperbolic distributions with index 1. Using the invariances of the NIG it is given by the four-parameter formula

$$f_j(x, \alpha, \beta, \delta, \mu) = \frac{\alpha\delta \, e^{\delta\gamma} K_1 \left(\alpha\sqrt{\delta^2 + (x - \mu)^2} \right)}{\pi\sqrt{\delta^2 + (x - \mu)^2}} \, e^{\beta(x - \mu)}, \quad j = 1, 2, \tag{42}$$

where, α measures how heavy the tail of the distribution is, β measures how skew it is, δ is a scaling parameter and μ determines the location (center) of the distribution, $\gamma = \sqrt{\alpha^2 - \beta^2}$. K_1 is the modified Bessel's function of the second kind with index 1. Now the 1st moment of the velocity differences is

$$E(\delta_j u) = E([u(x+s,\cdot)-u(x,\cdot)]\cdot r) = E(|u(x+s,\cdot)-u(x,\cdot)||r|\cos(\theta))$$
$$= \int_{\infty}^{\infty} (xf_j)(x,\alpha,\beta,\delta,\mu)dx, \tag{43}$$

where $j=1$, if $r=\hat{s}$ is the longitudinal direction (that is the direction along the lag vector s), and $j=2$, if $r=\hat{t}$ where $t \perp s$ is a transversal direction, $\hat{r}$ and $\hat{t}$ being unit vectors. θ is the angle between the vectors $[u(x+s,\cdot)-u(x,\cdot)]$ and r, and the absolute value of the former is the reason why the angle derivatives wash out in (39). The PDF is symmetric in the transversal direction, then $\beta=\mu=0$. In that case there are only two independent adjustable parameters, α is the exponential decay at $x=\pm\infty$ and δ is the "peakedness" at the origin. In the nonsymmetric case, there are two more independent adjustable parameters, the skewness parameter β and the centering parameter μ.

The PDF for the velocity increments has the asymptotics,

$$f_j \sim \frac{\delta e^{\delta\gamma}}{\pi} \frac{e^{\beta(x-\mu)}}{(\delta^2+(x-\mu)^2)}$$

for $(x-\mu)$ small. This is the algebraic (rational) cusp at the origin. The exponential tails are,

$$f_j \sim \frac{\sqrt{2}\delta\alpha e^{\delta\gamma-\beta\mu}}{\pi^{3/2}} \frac{e^{-\alpha|x|+\beta x}}{|x|^{3/2}}$$

for $|x|$ large.

The exponential tails of the PDF are caused by occasional sharp velocity gradients (rounded-off shocks), whereas the cusp at the origin is caused by the random and gentile fluid motion in the center of the ramps leading up to the sharp velocity gradients, see Kraichnan [24].

For large values of the lag variable, the NIG distribution must also approximate a Gaussian. It turns out to do just that. Letting $\alpha,\delta\to\infty$, in the formulas for $f_j(x)$ above, in such a way that $\delta/\alpha\to\sigma$, we get that

$$f_j \to \frac{e^{-\frac{(x-\mu)^2}{2\sigma}}}{\sqrt{2\pi\sigma}} e^{\beta(x-\mu)}.$$

12 Comparison with Simulations and Experiments.

We now compare the above PDFs with the PDFs found in simulations and experiments, using the first moment $g_j(x)=(xf_j)(x,\alpha,\beta,\delta,\mu)$, where f_j, $j=1,2$ are the

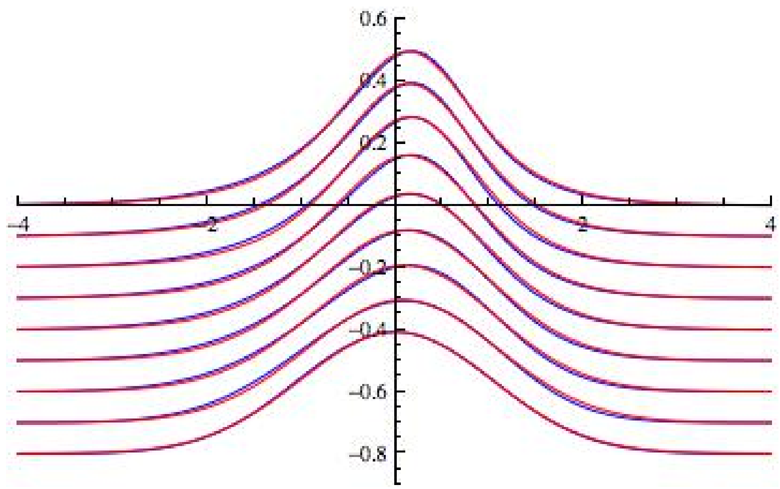

Figure 1: The PDF from simulations and fits for the longitudinal direction. The PDFs for increasing values of the lag variable are displaced downward. The last PDF looks distinctly Gaussian.

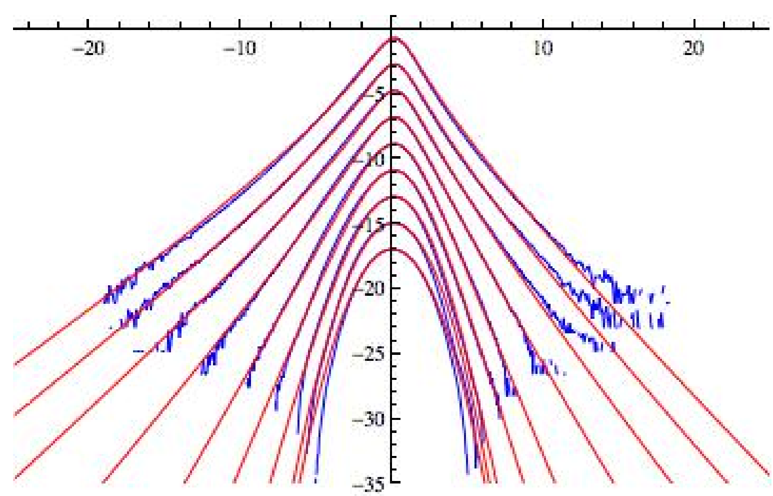

Figure 2: The log of the PDF from simulations and fits for the longitudinal direction, compare Fig. 4.5 in [40]. Again the logs of PDFs for increasing values of the lag variable are displaced downward. The last ones look Gaussian.

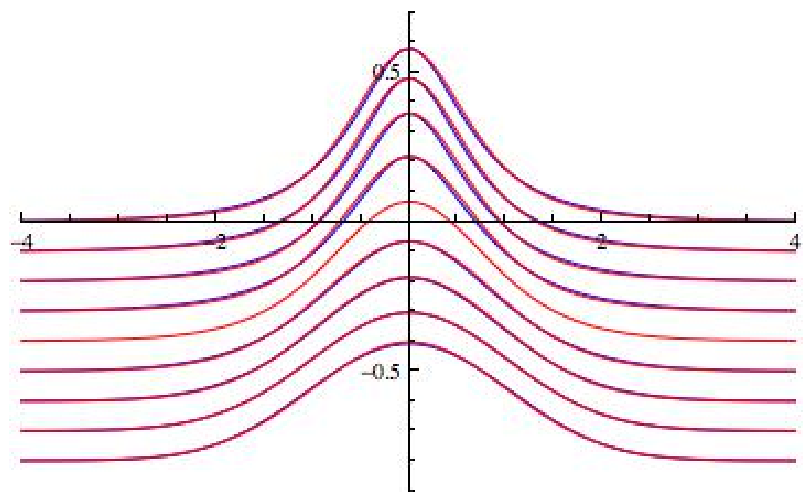

Figure 3: The PDF from simulations and fits for a transversal direction. The PDFs for increasing values of the lag variable are displaced downward. The last PDF looks distinctly Gaussian.

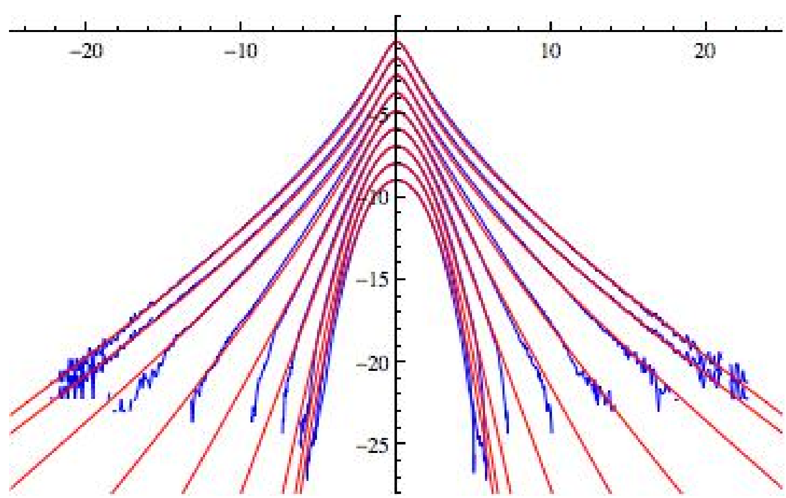

Figure 4: The log of the PDF from simulations and fits for the a transversal direction, compare Fig. 4.6 in [40]. Again the logs of PDFs for increasing values of the lag variable are displaced downward. The last ones look Gaussian and all of them are symmetric and centered at 0.

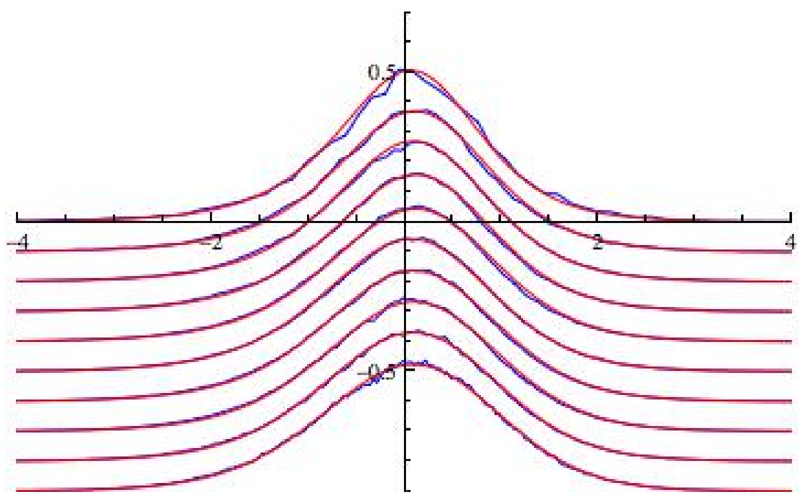

Figure 5: The PDF from experiments and fits. The PDFs for increasing values of the lag variable are displaced downward.

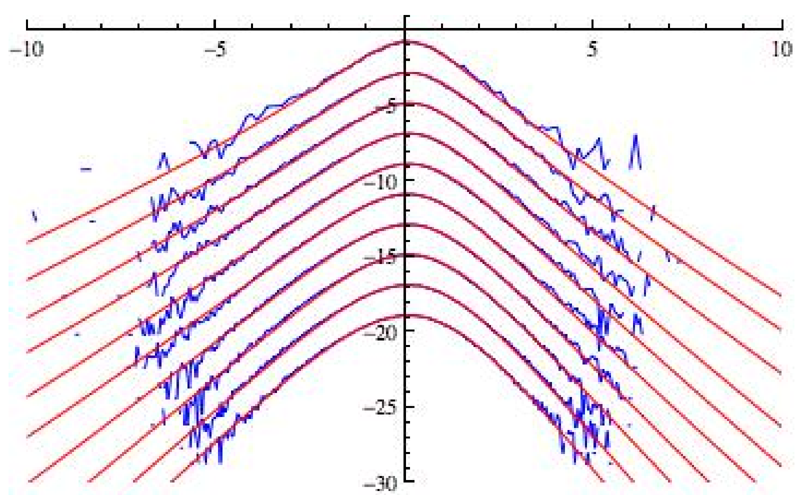

Figure 6: The log of the PDF from experiments and fits. Again the logs of PDFs for increasing values of the lag variable are displaced downward.

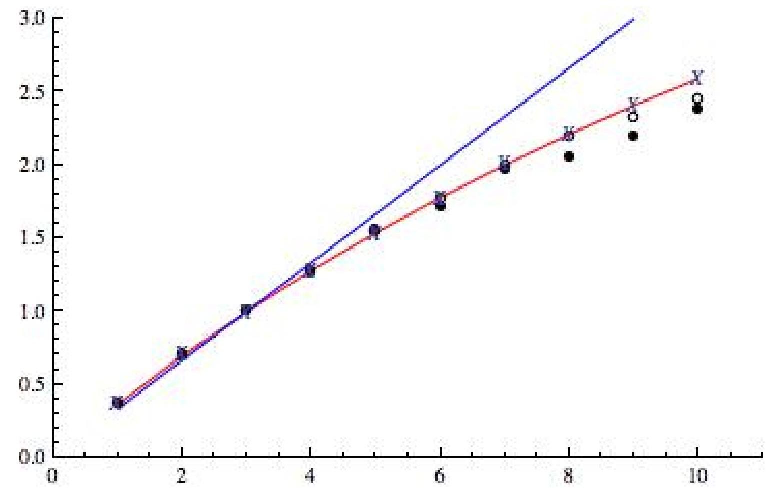

Figure 7: The exponents of the structure functions as a function of order, theory or Kolmogorov-Obukov-She-Leveque scaling (red), experiments (disks), dns simulations (circles), from [14], and experiments (X), from [35]. The Kolomogorov-Obukhov '41 scaling is also shown as a blue line for comparion.

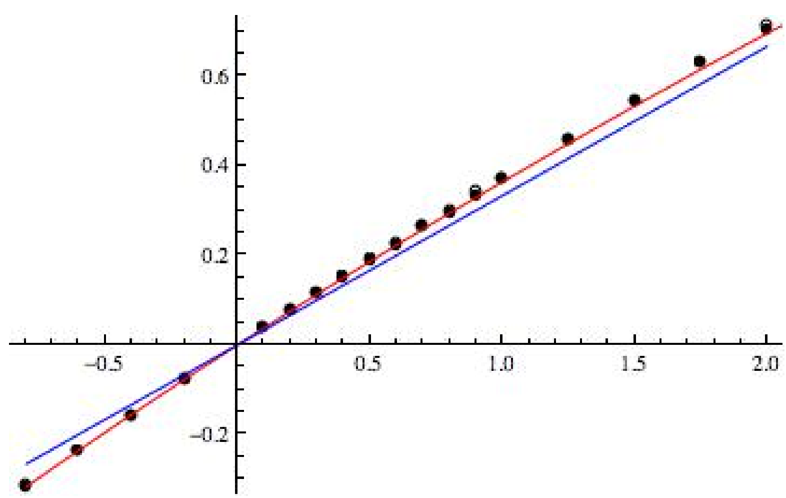

Figure 8: The exponents of the structure functions as a function of order $(-1, 2]$, theory or Kolmogorov-Obukov-She-Leveque scaling (red), experiments (disks), dns simulations (circles), from [14]. The Kolmogorov-Obukov '41 scaling is also shown as a blue line for comparion.

PDFs in formula (42). Because of the discrete jump measure (23) all the higher moments come with their own PDF. The PDF for the pth moment is given by the formula

$$f^p_{j\ (\alpha,\beta,\delta,\mu)(p)}(x) = \frac{\alpha\delta\, e^{\delta\gamma} K_1\left(\alpha\sqrt{\delta^2+(x-\mu)^2}\right)}{\pi\sqrt{\delta^2+(x-\mu)^2}}\, e^{\beta(x-\mu)}, \tag{44}$$

where $\gamma = \sqrt{\alpha^2-\beta^2}$, K_1 is the modified Bessel's function of the second kind with index 1, similar to (42). The density of the pth moment itself is

$$x^p f^p_{j\ (\alpha,\beta,\delta,\mu)(p)}(x) = \frac{\alpha^{1-p}\delta\, e^{\delta\gamma} K_1\left(\alpha\sqrt{\delta^2+(x-\mu)^2}\right)}{\pi(\delta^2+(x-\mu)^2)^{(1-p)/2}}\, e^{\beta(x-\mu)}, \tag{45}$$

where $j=1$, for the longitudinal and $j=2$ for the transverse component, as in (42). All the four parameters α,β,δ,μ are functions of p because of intermittency.

If the first four moments in (41) are given, then the four parameters in the NIG distribution can be computed directly. However, this is probably not the best way to do so. Firstly, this would only give the parameters for the first four moments and the parameters for the higher moments would have to be computed separately. Secondly, since both the longitudinal and the transverse moments can be measured, see Formula (43), giving the first four moments may overdetermine the four parameters in NIG. A better method is to give both the longitudinal and transverse measurements for two moments. This will determine the four parameters in NIG and give the NIG for these two moments. One is actually giving the NIG of the projection onto these two moments in moments space. From a theoretical point of view it makes sense to always give the measurements for the third moment, because it does not have any intermittency corrections, corresponding to Kolmogorov's $4/5$ law. Thus one can say given the longitudinal and transverse measurements for the third moment, the PDF (NIG) for every moment is determined by the longitudinal and transverse measurements for that moment. However, it may depend on the experiment whether this is the most practical projection.

The direct Navier-Stokes (DNS) simulations, in Figures 1 to 4, were provided by Michael Wilczek from his Ph.D. thesis, see [40]. The simulations are plotted in blue and the fits in red. The experimental results in Figures 5 and 6 are from the particle tracking experiments by Eberhard Bodenschatz group. The PDFs of Eulerian velocity differences are obtained from the instantaneous particle velocities by conditioning on given spatial separations, see Xu, Ouellette and Bodenschatz

[42]. In each case the fit was checked by computing the normalized log-likelihood function. First the data point zero or close to zero were removed and then the normalized log-likelihood function computed for the remaining points.The experimental results are plotted in blue and the fits in red. The experimental results in Figures 7 and 8 are from Sreenivasan and Dhruva [38] for the high Reynolds number atmospheric turbulence. The numbers plotted are from Table 2 in [14] where both experimental and simulations results are compared. We plotted the numbers from the latter simulation (1024^3) in the Table. We thank all of these researchers for the permission to use their results to compare with the theoretically computed PDFs. The NIG distribution, was used by Barndorff-Nilsen et al. [7] to obtain fits to the PDFs for three different experimental data sets.

13 Description of Simulations and Experiments

First we described the simulations in the Ph.D. thesis of Michael Wilczek following [40]. The DNS data was produced by a standard pseudospectral code with periodic boundary conditions at a Taylor-based Reynolds number of 112. The simulations were run in a statistically stationary state with a large-scale forcing that preserves the kinetic energy of the flow and delivers approximately homogeneous isotropic turbulence. For more details we refer the reader to Michael Wilczek's Ph.D. thesis [40] and to [41].

The experiment by Xu, Ouellette and Bodenschatz is described in their paper [42]: The turbulence is generated in a closed cylindrical chamber containing roughly 0.1 m^3 of water using counterrotating disks (French washing machine). The flow was seeded with transparent polystyrene microspheres with a diameter of $25\mu m$ (smaller than or comparable to the smallest turbulent length scale) and a density 1.06 times that of water. These particles have previously been shown to act as passive tracers in this flow. The microspheres were illuminated by two pulsed Nd:YAG lasers, and their motion was recorded in three dimensions by three high-speed cameras at rates of up to 27 000 frames per second so that the smallest turbulent time scales were well resolved. The trajectories of individual tracer particles were reconstructed using particle tracking algorithms. Once the raw particle tracks were obtained, Lagrangian velocities were obtained by convolution with a Gaussian smoothing and differentiating kernel. The smoothing operation works as a filter to suppress the measurement noise while the differentiation operation gives the derivative of the filtered signal.

The data from [38] consists of a series of measurements in atmospheric tur-

U	u'	ε	η	λ	R_λ
$7.6\ ms^{-1}$	$1.36\ ms^{-1}$	$0.032\ m^2s^{-3}$	$0.57\ mm$	$11.4\ mm$	$10,340$

Table 2: Some relevant parameters for the atmospheric data. Here, U is the mean speed, u' is the root-mean-square velocity, ε is the mean rate of energy dissipation, η and λ are the Kolmogorov and Taylor microscales, respectively, and $R_\lambda = u\lambda/\nu$, ν being the kinematic viscosity of air at the measurement temperature.

bulence at Talylor microscale Reynolds number $\sim \sqrt{15R}$ ranging between 10,000 and 20,000. The Taylor frozen hypothesis is used but it was verified by comparison with true spatial data obtained from two probes separated by a known streamwise distance, see [38]. The parameter values are listed in Table 2, see [14].

Hotwire measurements were made in the atmospheric surface layer at a height of 35 m above the ground using a standard meteorological tower at Brookhaven National Laboratory. The tower itself presented very little obstacle to the wind because of its low solidity. The dataset analyzed here is part of a more comprehensive batch of data obtained at the tower. The hotwire, 0.7 mm in length and 0.5 μm in diameter, was placed facing the wind, about two meters away from the tower. (For monitoring the wind direction, the tower was equipped with a vane anemometer placed two meters away from the measurement station.) The calibration was performed in situ using a TSI calibrator and checked later in a windtunnel. The signals were low-pass filtered at 5 kHz and sampled at 10 kHz. The anemometer and signal conditioners were placed nearby at the height of measurement, and the conditioned signal was transmitted to the ground and digitized using a 12-bit A/D converter. Typical data records contained between 10 and 40 million samples, during which time the wind direction and its mean speed were deemed acceptably constant. More details are given in Dhruva [15], but the essential features for this particular set of data are listed in Table 2. The wind conditions were somewhat unstable.

14 Conclusion

We have seen that the Navier-Stokes equation for all but the largest scales in turbulent flow can be expressed as a stochastic Navier-Stokes equation (7). The stochastic forcing results from instabilities of the flow that magnifies small ambient noise and saturates its growth into large stochastic forcing. This has been modeled before by a Reynolds decomposition and by a coarse graining of the flow. The stochastic force is generic and is determined by the general principles of probability with a minimum of physical inputs. It consists of two components additive noise and multiplicative noise and the additive component is determined by the central limit theorem and the large deviation principle. The physical input is that these two term must produce similar scalings because they are caused by the same dissipative processes. This determines the rate in the large deviation principle. The multiplicative noise multiplies the fluid velocity and models jumps (vorticity concentrations) in the velocity gradient. It is expressed by a generic Poisson process where only the rate needs to be given. This rate is determined by the spectral analysis of the (linearized) Navier-Stokes operator and the requirement, following [35], that the dimension of the most singular vorticity structure (filaments) is one. Thus the stochastic forcing is generic and determined with two mild physical inputs.

The stochastic Navier-Stokes equation can be expressed as an integral equation (8) and the log-Poissonian processes found by She and Leveque and explored by She and Waymire and Dubrulle are produced from the multiplicative noise by the Feynmann-Kac formula. This give a satisfying mathematical derivation of the intermittency phenomena that had earlier been derived from impirical considerations. Moreover, the integral equations show how the Navier-Stokes evolution and the log-Poissonian intermittency processes act on the dissipation processes to product the intermittency in the dissipation. This is a mathematical derivation of the experimental observation that intermittent dissipation processes accompany intermittent velocity variations. Using the integral equation we get a lower estimate on all the structure functions of the velocity differences in turbulence. The evidence from simulations and experiments is that this lower bound is reached in turbulent flow. Why the inertial cascade achieves this maximal efficiency in the energy transfer remains to be explained.

We then built on Hopf's [18] ideas to compute the invariant measure of turbulent flow. This measure can be computed because it solves a linear functional differential equation, see [33]. It turns out to be an infinite-dimensional Gaussian multiplied by a (discrete) Poisson distributions. This Poisson distribution corresponds to the intermittency and the log-Poisson processes. Then by taking the trace of the invariant measure we get the PDF of the velocity differences. We first derive the functional differential equation (PDE) for the PDF and then show that there are infinitely many PDF each corresponding to a particular moment, because of the intermittency corrections. The PDE (38) for the sequence of PDFs can also be solved and the PDF turn out to be the normalized inverse Gaussian (NIG) distributions of Barndorff-Nilsen [5]. Their parameters are easly computed and we see how to do this for both simulations and experiments.

It is interesting to notice that although the solution of the Navier-Stokes equation may not be unique or smooth the invariant measure of the velocity differences (35) is still well defined by Leray's [25] existence theory. Moreover, different velocities produce equivalent measures so the statistical observables of turbulence are unique although the turbulent velocity may not be.

Acknowledgments The author would like to acknowledge a large number of colleagues that the results in this paper have been discussed with and have provided valuable insights. The include Ole Barndorff-Nilsen and Jurgen Schmiegel in Aarhus, Henry McKean, K. R. Sreenivasan and R. Varadhan in New York, Z-S Zhe in Beijing, Ed Waymire in Oregon, E. Bodenschatz and H. Xu in Gottingen, Michael Wilczek in Munster and M. Sørensen in Copenhagen. He also benefitted from conversations with J. Peinke, M. Oberlack, E. Meiburg, B. Eckhardt, S. Childress, L. Biferale, L-S. Yang, A. Lanotto, K. Demosthenes, M. Nelkin, A. Gylfason, V. L'vov and many others. This research was supported in part by the Project of Knowledge Innovation Program (PKIP) of Chinese Academy of Sciences, Grant No. KJCX2.YW.W10, whose support is gratefully acknowledged.

References

[1] F. Anselmet, Y. Gagne, E. J. Hopfinger, and R. A. Antonia. High-order velocity structure function sin turbulent shear flows. *J. Fluid Mech.*, 14:63–89, 1984.

[2] A. Babin, A. Mahalov, and B. Nicolaenko. Long-time averaged Euler and Navier-Stokes equations for rotation fluids. *In Structure and Dynamics of non-linear waves in Fluids, 1994 IUTAM Conference, K. Kirehgassner and A. Mielke (eds), World Scientific*, page 145157, 1995.

[3] A. Babin, A. Mahalov, and B. Nicolaenko. Global splitting, integrability and regularity of 3d Euler and Navier-Stokes equation for uniformely rotation fluids. *Eur. J. Mech. B/Fluids*, 15(2):08312, 1996.

[4] O. E. Barndorff-Nilsen. Exponentially decreasing distributions for the logarithm of the particle size. *Proc. R. Soc. London*, A 353:401–419, 1977.

[5] O. E. Barndorff-Nilsen. Processes of normal inverse Gaussian type. *Finance and Stochastics*, 2:41–68, 1998.

[6] O. E. Barndorff-Nilsen, P. Blæsig, and M Sorensen. Parametric modelling of turbulence. *Phil. Trans. R. Soc. Lond. A*, 322:435–455, 1990.

[7] O. E. Barndorff-Nilsen, P. Blaesild, and Jurgen Schmiegel. A parsimonious and universal description of turbulent velocity increments. *Eur. Phys. J. B*, 41:345–363, 2004.

[8] P. S. Bernard and J. M. Wallace. *Turbulent Flow*. John Wiley & Sons, Hoboken, NJ, 2002.

[9] R. Bhattacharya and E. C. Waymire. *Stochastic Processes with Application*. John Wiley, New York, 1990.

[10] P. Billingsley. *Probability and Measure*. John Wiley, New York, 1995.

[11] B. Birnir. Turbulence of a unidirectional flow. *Proceedings of the Conference on Probability, Geometry and Integrable Systems, MSRI, Dec. 2005 MSRI Publications, Cambridge Univ. Press*, 55, 2007. Available at http://repositories.cdlib.org/cnls/.

[12] B. Birnir. The Existence and Uniqueness and Statistical Theory of Turbulent Solution of the Stochastic Navier-Stokes Equation in three dimensions, an overview. *Banach J. Math. Anal.*, 4(1):53–86, 2010. Available at http://repositories.cdlib.org/cnls/.

[13] B. Birnir. *The Kolmogorov-Obukhov Theory of Turbulence*. Springer, New York, 2012.

[14] S. Y. Chen, B. Dhruva, S. Kurien, K. R. Sreenivasan, and M. A. Taylor. Anomalous scaling of low-order structure functions of turbulent velocity. *Journ. of Fluid Mech.*, 533:183–192, 2005.

[15] B. Dhruva. *An experimental study of high-Reynolds-number turbulence in the atmosphere*. Ph.D. Thesis Yale University, New Haven, CT, 2000.

[16] B. Dubrulle. Intermittency in fully developed turbulence: in log-Poisson statistics and generalized scale covariance. *Phys. Rev. Letters*, 73(7):959–962, 1994.

[17] U. Frisch. *Turbulence*. Cambridge Univ. Press, Cambridge, 1995.

[18] E. Hopf. Statistical hydrodynamics and functional calculus. *J. Rat. Mech. Anal.*, 1(1):87–123, 1953.

[19] T. Kato. *Perturbation Theory for Linear Operators*. Springer, New York, 1976.

[20] A. N. Kolmogorov. Dissipation of energy under locally istotropic turbulence. *Dokl. Akad. Nauk SSSR*, 32:16–18, 1941.

[21] A. N. Kolmogorov. The local structure of turbulence in incompressible viscous fluid for very large Reynolds number. *Dokl. Akad. Nauk SSSR*, 30:9–13, 1941.

[22] A. N. Kolmogorov. A refinement of previous hypotheses concerning the local structure of turbulence in a viscous incompressible fluid at high Reynolds number. *J. Fluid Mech.*, 13:82–85, 1962.

[23] R. H. Kraichnan. On Kolmogorov's inertial-range theories. *J. Fluid Mech.*, 62:305–330, 1974.

[24] R. H. Kraichnan. Turbulent cascade and intermittency growth. *In Turbulence and Stochastic Processes, eds. J. C. R. Hunt, O. M. Phillips and D. Williams, Royal Society*, pages 65–78, 1991.

[25] J. Leray. Sur le mouvement d'un liquide visqueux emplissant l'espace. *Acta Math.*, 63(3):193–248, 1934.

[26] H. P. McKean. Turbulence without pressure: Existence of the invariant measure. *Methods and Applications of Analysis*, 9(3):463–468, 2002.

[27] A. M. Obukhov. On the distribution of energy in the spectrum of turbulent flow. *Dokl. Akad. Nauk SSSR*, 32:19, 1941.

[28] A. M. Obukhov. Some specific features of atmospheric turbulence. *J. Fluid Mech.*, 13:77–81, 1962.

[29] B. Oksendal. *Stochastic Differential Equations*. Springer, New York, 1998.

[30] B. Oksendal and A. Sulem. *Applied Stochastic Control of Jump Diffusions*. Springer, New York, 2005.

[31] L. Onsager. Statistical hydrodynamics. *Nuovo Cimento.*, 6(2):279–287, 1945.

[32] S. B. Pope. *Turbulent Flows*. Cambridge Univ. Press, Cambridge UK, 2000.

[33] G. Da Prato. *An Introduction of Infinite-Dimensional Analysis*. Springer Verlag, New York, 2006.

[34] R. Renzi, S. Ciliberto, C. Baudet, F. Massaioli, R. Tripiccione, and S. Succi. Extended self-similarity in turbulent flow. *Phys. Rev. E*, 48(29):401 – 417, 1993.

[35] Z-S She and E. Leveque. Universal scaling laws in fully developed turbulence. *Phys. Rev. Letters*, 72(3):336–339, 1994.

[36] Z-S She and E. Waymire. Quantized energy cascade and log-poisson statistics in fully developed turbulence. *Phys. Rev. Letters*, 74(2):262–265, 1995.

[37] Z-S She and Zhi-Xiong Zhang. Universal hierarchial symmetry for turbulence and general multi-scale fluctuation systems. *Acta Mech Sin*, 25:279–294, 2009.

[38] K. R. Sreenivasan and B. Dhruva. Is there scaling in high- Reynolds-number turbulence? *Prog. Theor. Phys. Suppl.*, 103–120, 1998.

[39] S. R. S. Varadhan. *Large Deviations and Applications*. SIAM, Philadelphia,PA, 1884.

[40] M. Wilczek. *Statistical and Numerical Investigations of Fluid Turbulence*. PhD Thesis, Westfälische Wilhelms Universität, Münster, Germany, 2010.

[41] M. Wilczek, A. Daitche, and R. Friedrich. On the velocity distribution in homogeneous isotropic turbulence: correlations and deviations from Gaussianity. *J. Fluid Mech.*, 676:191–217, 2011.

[42] H. Xu, N. T. Ouellette, and E. Bodenschatz. Multifractal dimension of Lagrangian turbulence. *Phys. Rev. Letters*, 96:114503, 2006.